DOI: 10.1002/chem.200601073

Synthetic, Structural, and Theoretical Investigations of Alkali Metal Germanium Hydrides—Contact Molecules and Separated Ions

Weijie Teng, Damian G. Allis,* and Karin Ruhlandt-Senge*[a]

Dedicated to Professor Glen B. Deacon on the occasion of his 70th birthday

Abstract: The preparation of a series of crown ether ligated alkali metal (M = K, Rb, Cs) germyl derivatives M(crown ether)$_n$GeH$_3$ through the hydrolysis of the respective tris(trimethylsilyl)germanides is reported. Depending on the alkali metal and the crown ether diameter, the hydrides display either contact molecules or separated ions in the solid state, providing a unique structural insight into the geometry of the obscure GeH$_3^-$ ion. Germyl derivatives displaying M–Ge bonds in the solid state are of the general formula [M([18]crown-6)(thf)GeH$_3$] with M = K (**1**) and M = Rb (**4**). The compounds display an unexpected geometry with two of the GeH$_3$ hydrogen atoms closely approaching the metal center, resulting in a partially inverted structure. Interestingly, the lone pair at germanium is not pointed towards the alkali metal, rather two of the three hydrides are approaching the alkali metal center to display M–H interactions. Separated ions display alkali metal cations bound to two crown ethers in a sandwich-type arrangement and non-coordinated GeH$_3^-$ ions to afford complexes of the type [M(crown ether)$_2$][GeH$_3$] with M = K, crown ether = [15]crown-5 (**2**); M = K, crown ether = [12]crown-4 (**3**); and M = Cs, crown ether = [18]crown-6 (**5**). The highly reactive germyl derivatives were characterized by using X-ray crystallography, ^{1}H and ^{13}C NMR, and IR spectroscopy. Density functional theory (DFT) and second-order Møller–Plesset perturbation theory (MP2) calculations were performed to analyze the geometry of the GeH$_3^-$ ion in the contact molecules **1** and **4**.

Keywords: alkali metals · density functional calculations · germanium · hydrides · structure elucidation

Introduction

KGeH$_3$ was first obtained in 1934 by treatment of potassium with GeH$_4$ in liquid ammonia,[1,2] with subsequent work including the heavier alkali metals[3] and solvent systems other than ammonia.[4] The continued interest in these compounds originates from their potential in photovoltaic devices; with recent work focusing on the improved conversion of sunlight into electricity.[5] In an effort to improve the conversion rate of amorphous silicon, the introduction of germanium by means of MGeH$_3$ (M = alkali metals) resulted in an optimized use of the solar spectrum by including longer wavelength radiation, leading to a significant increase in efficiency.

The GeH$_3^-$ ion is also of interest in a more fundamental context, since the examination of the geometries in the Group 14 moieties CH$_3^-$, SiH$_3^-$, GeH$_3^-$, and SnH$_3^-$ provides important information on structure and bonding trends.

Despite technological applications and the desire to improve fundamental insight on structure and bonding, only scarce information exists for the GeH$_3^-$ ion,[1–4,6–9] with structural details limited to saltlike germyl species.[3] The potassium and rubidium species crystallize in a NaCl lattice, while the cesium compound crystallizes in the TlI structure type.[3] While these studies provide an overall insight into cation and anion arrangements, no information was obtained on the germyl anion geometry, since the anions rotate on their lattice position and thus only show average values. The anion size was predicted on the basis of structural comparisons, leading to the assignment of an effective radius for the GeH$_3^-$ ion of 2.29 Å.[3] Geometrical data for the GeH$_3^-$ ion

[a] Dr. W. Teng, Dr. D. G. Allis, Prof. Dr. K. Ruhlandt-Senge
Department of Chemistry
1-014 Center for Science and Technology, Syracuse University
Syracuse, New York 13244-4100 (USA)
Fax: (+1) 315-443-4070
E-mail: damian@somewhereville.com
kruhland@syr.edu

Supporting information for this article is available on the WWW under http://www.chemeurj.org/ or from the author.

were obtained by NMR spectroscopy, with the prediction of a pyramidal geometry with H-Ge-H angles of $92.5 \pm 4.0°$.[3] Well-defined germyl derivatives were obtained by treating transition-metal carbonyls with $KGeH_3$. GeH_3^- was found to replace one carbonyl functionality, affording $[N(CH_3)_4][\eta\text{-}CH_3C_5H_4Mn(CO)_2GeH_3]$,[10] $[PPh_4][Cr(CO)_5GeH_3]$,[11] $[PPh_4][V(Cp)(CO)_2GeH_3]$ (Cp = cyclopentadienide),[12] $[PPh_4][M(CO)_nGeH_3]$ (M = Mo, $n=5$; M = W, $n=5$; M = Ni, $n=3$),[12] and $[PPh_4][Mo(CO)_2PPh_3GeH_3]$.[12] Replacement of the initially formed potassium salts by the larger PPh_4^+ or NMe_4^+ ions afforded complexes with increased stability. However, in analogy with the alkali metal species mentioned above, geometrical details of the GeH_3^- moieties were not available, due to difficulties in locating the hydrogen atoms.

Other compounds displaying a Ge–H moiety contain a reduced amount of hydridic hydrogen bound to germanium. Examples include the transition-metal species $[V(Cp)_2(C_6F_5)_2GeGeH(C_6F_5)_2]$,[13] $[Mo(Cp)(CO)_2P(CH_3)_3GeCl_2H]$,[14] $[Yb(thf)_4(GePh_3(\mu\text{-}H))_2]$,[15,16] $[Fe_2(Cp)_2(CO)_2(\mu\text{-}CO)(\mu\text{-}Ge)tBuH]$,[17] $[MoH(Et_4P_2(CH_2)_2)_2GePhH_2]$,[18] and $[MoH(Et_4P_2(CH_2)_2)_2GePh_2H(\mu\text{-}H)]$.[18] Main-group derivatives are limited to $[\{(tBuMe_2Si)_2HGeLi\}_2]$, obtained by the reaction of $(tBuMe_2Si)_2GeH_2$ with *t*BuLi in THF,[19] and $[M_2\{Ge(H)Ar'\}_2]$ (M = Li, Na, K; $Ar' = C_6H_3\text{-}2,6\text{-}(C_6H_3\text{-}2,6\text{-}iPr_2)_2$), prepared by the treatment of Ar′(H)GeGe(H)Ar′ with the metals in toluene.[20]

We here present the first family of discrete alkali metal germyl derivatives. The introduction of crown ether improves the solubility, allowing detailed characterization. Examples presented include two contact molecules [M([18]crown-6)(thf)(GeH_3)], M = K (**1**) and M = Rb (**4**), as well as the separated ions $[M(crown)_2][GeH_3]$ M = K, donor = [15]crown-5 (**2**); M = K, donor = [12]crown-4 (**3**); and M = Cs, donor = [18]crown-6 (**5**). The mechanism of formation for compounds **1**–**5** was evaluated by treating the previously published $[K([18]crown\text{-}6)Ge(SiMe_3)_3]$[21,22] with deuteriumoxide.

Results and Discussion

Preparation and reactivity: M(crown ether)GeH_3 (M = K, Rb, and Cs, donor = [18]crown-6, [15]crown-5, [12]crown-4) derivatives were prepared by very slow addition of degassed water (water-laced THF stock solutions) to the parent M(crown ether)$Ge(SiMe_3)_3$ (M = K, Rb, and Cs, donor = [18]crown-6, [15]crown-5, [12]crown-4). A potential mechanism of formation involves protonation of the germanides by water (or D_2O), affording H/DGe$(SiMe_3)_3$ [Eq. (1)]. $KGe(SiMe_3)_3$ and H/DGe$(SiMe_3)_3$ undergo a trimethylsilane transfer to yield KGeH/D$(SiMe_3)_2$ and $Ge(SiMe_3)_4$, a side product always observed in samples of $MGe(SiMe_3)_3$ (M = K, Rb, Cs) upon standing over a period of time [Eq. (2)]. The resulting potassium hydroxide may cause a nucleophilic attack on silicon, which under formation of a five-coordinate transition state affords KGeH/$D_2(SiMe_3)$ and trimethylsiloxide [Eqs. (3) and (4)]. Repetition of this sequence results in the hydrides **1**–**5**. Literature evidence supports the validity of these proposed reaction sequences,[23–28] with protonation as the first step suggested by Marschner on silanides, in which the treatment of $KSi(SiMe_3)_3$ with acid afforded $HSi(SiMe_3)_3$.[26] Apparently, for the silanides, water appears not to be a strong enough protonating agent, but the more reactive germanide easily reacts with the weaker acids water and D_2O.

$$KGe(SiMe_3)_3 + H_2O \rightarrow HGe(SiMe_3)_3 + KOH \quad (1)$$

$$KGe(SiMe_3)_3 + HGe(SiMe_3)_3 \rightarrow KGeH(SiMe_3)_2 + Ge(SiMe_3)_4 \quad (2)$$

$$KGeH(SiMe_3)_2 + KOH \rightarrow KGeH_2SiMe_3 + KOSiMe_3 \quad (3)$$

$$KGeH_2SiMe_3 + KOH \rightarrow KGeH_3 + KOSiMe_3 \quad (4)$$

The germyl derivatives were initially obtained inadvertently while preparing $[K([18]crown\text{-}6)Ge(SiMe_3)_3]$ derivatives by treatment of $Ge(SiMe_3)_4$ with alkali metal *tert*-butoxides [Eq. (5)]. The GeH_3^- derivatives were identified after the reaction vessel had been opened under argon to remove a few crystals for structural characterization. Subsequent bulk analysis by ^1H NMR spectroscopy upon removal of solvent indicated a smaller $[Ge(SiMe_3)_3]^-$ signal with respect to the initial spectra in addition to a broad signal between $\delta = 2$ and 3 ppm, later identified as Ge–H resonance. With the decrease in signal intensity for $[Ge(SiMe_3)_3]^-$, a signal for $Ge(SiMe_3)_4$ ($\delta = 0.31$ ppm) also appears and increases in intensity. The crystalline nature of the solid allowed for crystallographic characterization, indicating the formation of alkali metal germyl derivatives.

$$Ge(SiMe_3)_4 + MOtBu + n\,\text{donor} \rightarrow [M(\text{donor})_nGe(SiMe_3)_3] + Me_3SiOtBu \quad (5)$$

Initially believed to be the product of THF cleavage, an experiment involving the treatment of $Ge(SiMe_3)_4$ with KO*t*Bu and [18]crown-6 in an NMR tube under addition of anhydrous [D_8]THF was conducted. The reaction mixture was kept at room temperature and monitored over a period of several weeks. During this time, the ratio of $[Ge(SiMe_3)_3]^-$ and crown ether resonances remained constant; providing no indication for the formation of $KGe(SiMe_3)_2D$, $KGe(SiMe_3)D_2$, or $KGeD_3$. An alternative explanation to rationalize the formation of the target compounds involves hydrolysis, as observed upon opening the reaction vessel under argon while removing crystals for crystallographic analysis. This theory was assessed by introducing stoichiometric amounts of water or D_2O to the $KGe(SiMe_3)_3$ solution by means of D_2O-laced THF stock solutions of known concentration. These experiments required great care, since the rapid addition of H_2O/D_2O affords intractable, complex product mixtures and insoluble products. Water/D_2O as the source of hydrolysis was confirmed by the formation of

GeD_3^- (2.31 ppm), as identified by deuterium NMR spectroscopy.

The comparison of reactivity in compounds **1**–**5** shows $[K([12]crown\text{-}4)_2][GeH_3]$ (**3**), is most reactive. Exposure to air results in immediate formation of flames and smoke, making any characterization attempts very challenging. In contrast, $[K([15]crown\text{-}5)_2][GeH_3]$ (**2**), while still highly air sensitive, is less reactive. It appears that there is no significant difference in reactivity for contact molecules or separated ions, suggesting that the steric saturation of the metal centers and not the ion association is responsible for the observed reactivity trends. However, more detailed studies on related compounds are needed to provide more detailed data.

Spectroscopic studies: Compounds **1**–**5** were studied by ^1H and ^{13}C NMR spectroscopy, with respective data listed in the Experimental Section. The hydrides are clearly identified by their ^1H NMR spectra, with chemical shifts at $\delta =$ 2.30 (**1**), 3.06 (**2**), 3.06 (**3**), 2.61 (**4**), and 2.98 ppm (**5**). Previous transition-metal germyl derivatives display Ge–H chemical shifts between $\delta = 2$ and 4 ppm, thus in agreement with the signals observed for compounds **1**–**5**.[10,12] The analysis of chemical shifts indicates smaller values for the contact molecules **1** and **4**, with those for the separated ions closely clustered together, suggesting that the ion association observed in the solid state might be conserved in solution. This observation is in contrast to the tris(trimethylsilyl)silanides and germanides, for which virtually identical chemical shifts are observed for contact molecules and separated ions in the presence of an aromatic solvent, suggesting the formation of separated ions in all cases. An explanation for the differences in ion association trends in solution is provided by the steric and electronic effects evoked by the sterically demanding $SiMe_3$ substituents. The bulky ligand and proximity of the crown ether might be responsible for a metal–ligand bond weakening due to steric repulsion. Electronic stabilization of the $[E(SiMe_3)_3]^-$ (E = Si, Ge) moiety by the electropositive $SiMe_3$ substituents may further contribute to the easy formation of separated ions.

The presence of the GeH_3^- ion is also clearly indicated in the (solid-state) IR spectrum with broad signals at 1701, 1719, 1724, 1732, and 1708 for compounds **1**–**5**, respectively. These numbers agree with previously observed values between 1740–1755 cm^{-1} for the related compound $KGeH_{3-n}(SiH_3)_n$ ($n = 1$–3).[7]

Structural aspects: Crystallographic information and data collection parameters for compounds **1**–**5** are summarized in Table 1. Geometrical data for the compounds are listed in Table 2. Compounds **1** and **4** are contact molecules and will be described together.

$[K([18]crown\text{-}6)(thf)GeH_3]$ (**1**) and $[Rb([18]crown\text{-}6)(thf)GeH_3]$ (**4**) display very similar structures (for the sake of brevity only that of compound **4** is shown in Figure 1), with **1** containing two independent molecules per asymmetric unit. In both compounds, no crystallographically imposed symmetry is observed. Compounds **1** and **4** display a "pseudo-octahedral" metal environment composed of an [18]crown-6 macrocycle, arranged in an approximate equatorial plane, with a THF donor and a germyl anion in the axial positions, resulting in a metal coordination number of eight. The *trans* angles are 164.61(7) and 161.36(7)° in **1** and 162.0° in **4**. The arrangement of the crown ether in the equatorial plane is made possible by the narrow O-M-O angles, observed at 59.93°(9) (av) for **1** and 59.03°(2) (av) for **4**. Metal–germanium bond lengths are 3.671(1) and 3.630(1) Å for **1** and 3.731(1) Å for **4**. Potassium–oxygen ([18]crown-6) and rubidium–oxygen ([18]crown-6) distances range from 2.802(3) to 2.914(3) Å (**1**) and 2.847(5) to 2.970 (4) Å (**4**), while the metal–THF distances are 2.844(3) and 2.832(3) Å for **1**, and 3.079(4) Å for **4**. For both compounds the germyl hydrogen atoms could be located in the electron difference map and were included in the refinement by using constraints (DFIX in SHELXTL).[29] Ge–H distances are observed between 1.390 and 1.409 Å for **1** and 1.301 and

Table 1. Crystallographic data for compounds **1**–**5**.

	1	**2**	**3**	**4**	**5**
formula	$C_{16}H_{35}GeKO_7$	$C_{20}H_{43}GeKO_{10}$	$C_{16}H_{35}GeKO_8$	$C_{16}H_{35}GeO_7Rb$	$C_{24}H_{48}CsGeO_{12}$
M_r	451.13	555.23	467.13	497.50	734.12
a [Å]	13.85870(10)	12.6848(11)	40.7694(5)	13.8336(8)	13.2513(4)
b [Å]	9.96700(10)	12.6848(11)	7.623	9.9878(6)	13.2513(4)
c [Å]	16.9439(2)	16.985(2)	29.6746(4)	16.9893(9)	19.0577(7)
β [°]	107.2060(10)		97.4500(10)	107.4170(10)	
V [Å^3]	2235.71(4)	2733.0(5)	9144.93(17)	2239.7(2)	3346.47(19)
Z	4	4	16	4	4
space group	*Pc*	$I\bar{4}$	*C*2/*c*	*Cc*	*P*4/*n*
ρ_{calcd} [g cm^{-3}]	1.340	1.349	1.357	1.475	1.457
μ [mm^{-1}]	1.586	1.319	1.556	3.556	2.039
T [K]	95	99	95	91	91
2θ range [°]	3.08–50.00	4.00–50.44	2.02–50.00	5.02–56.66	3.74–52.78
independent reflns	7093	2472	7978	3848	3453
parameteres	470	155	675	329	174
*R*1/*wR*2 (all data)	0.0524/0.0825	0.0578/0.1638	0.0679/0.1173	0.0434/0.0968	0.0492/0.0999
*R*1/*wR*2 [$>2\sigma$]	0.0378/0.0774	0.0565/0.1632	0.0580/0.1120	0.0392/0.0949	0.0355/0.0918

Table 2. Selected bond lengths [Å] and angles [°] for compounds **1**–**5** and the corresponding germanides.

	M–Ge	M–donor (crown ether)	M–donor (THF)	Si-Ge-Si/H-Ge-H (av)	Ge–H	Ref.
[K([18]crown-6)(thf)GeH_3] (**1**)	3.630(10) 3.671(10)	2.797(3)-2.913(3)	2.833(3) 2.844(3)	101.4	1.385–1.405	[a]
[K([18]crown-6)$Ge(SiMe_3)_3$]	3.400(7)	2.768(2)-2.910(2)	NA[b]	100.9	NA	[20]
[K([15]crown-5)$_2$][GeH_3] (**2**)	NA	2.830(5)-2.993(6)	NA	100.4	1.027- 1.031	[a]
[K([15]crown−5)$_2$][$Ge(SiMe_3)_3$]	NA	2.88(2)-2.902(11)	NA	101.0	NA	[20]
[K([12]crown−4)$_2$][GeH_3] (**3**)	NA	2.652(6)-2.908(3)	NA	101.7	1.050–1.077	[a]
[Rb([18]crown-6)(thf)GeH_3] (**4**)	3.731(1)	2.847(5)-2.970(4)	3.079(4)	100.3	1.301–1.309	[a]
[Rb([18]crown-6)$Ge(SiMe_3)_3$]	3.480(1) 3.540(2)	2.842(4)-3.024(4)	NA	102.2	NA	[20]
[Cs([18]crown−6)$_2$][GeH_3] (**5**)	NA	3.174(2)-3.542(2)	NA	NA	NA	[a]
[Cs([18]crown−6)$_2$][$Ge(SiMe_3)_3$]	NA	3.153(3)-3.574(3)	NA	98.2	NA	[20]

[a] This work. [b] NA = not applicable.

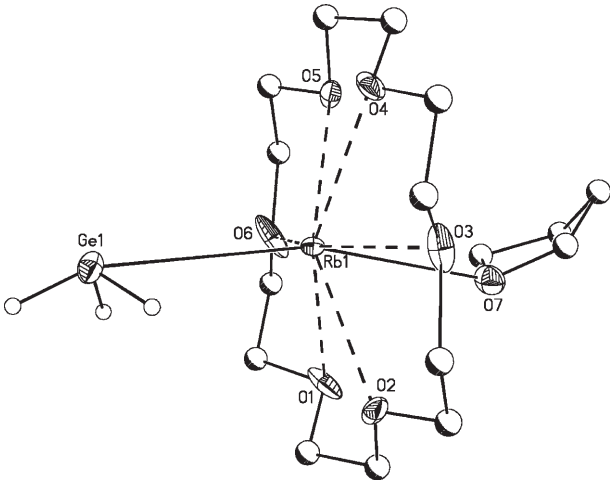

Figure 1. Graphical representation of compound **4**. Ellipsoids show 30% occupancy; hydrogen atoms, except those on GeH_3^-, have been removed for clarity.

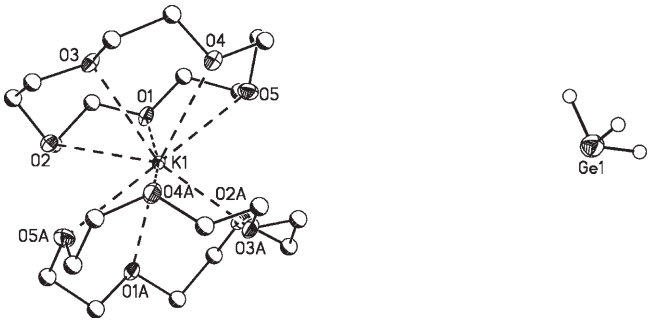

Figure 2. Graphical representation of compound **2**. Ellipsoids show 30% occupancy; hydrogen atoms, except those on GeH_3^-, have been removed for clarity.

1.309 Å for **4**. For both compounds the lone pair on the pyramidal Ge center does not point towards the alkali metal center, rather it is rotated away from the metal with an angle of about 90°. Accordingly, two Ge–H distances are closer to the metal than the third, the shortest values being between 3.260 and 3.341 Å for **1** and 3.442 and 3.449 Å for **4**. These distances are within the sum of van der Waals radii and can therefore be considered significant. The third hydrogen atom is quite distant from the metal center with distances of 4.936 and 4.962 Å for **1** and 4.978 Å for **4**. The orientation of the GeH_3^- ion towards the alkali metal/crown moiety is also expressed by the M-Ge-H angles, with two narrow and one wider angles. The environment at the GeH_3^- moieties is pyramidal with H-Ge-H angles ranging between 99 and 104°.

Compound **2**, shown in Figure 2, contains individual cations and anions, separated by 14.54 Å. The potassium cation is surrounded in a sandwich-type fashion by two [15]crown-5 macrocycles, resulting in a metal coordination number of ten and potassium–oxygen bond distances between 2.830(5) and 2.993(6) Å. The Ge–H distances range between 1.027 to 1.031 Å (hydrogen positions located in the electron difference map and inserted into refinement using restraints). The germyl geometry is distinctly pyramidal. Similar to **2**, compound **3** contains separated ions, apart from each other by at least 7.09 Å. The compound also contains two independent molecules in each asymmetric unit. Two crown ether molecules bind to the potassium cation in a sandwich-type fashion, resulting in a coordination number of eight and potassium–oxygen distances between 2.652(6) and 2.908(3) Å. Ge–H distances (hydrogens located in electron density map) are between 1.050 and 1.077 Å, the GeH_3^- geometry is pyramidal with H-Ge-H angles between 99–104°. Compound **5** contains ions separated by 8.08 Å and 8.01 Å. Each asymmetric unit contains two independent molecules. Each cation is surrounded by two [18]crown-6 macrocycles, resulting in a coordination number of twelve and cesium–oxygen distances between 3.174(2) and 3.542(2) Å. Hydrogen atoms in the anion could not be located or placed on calculated positions, since the germanium atom lies on a center of symmetry.

Among the alkali metal germyls **1**–**5**, both contact molecules (**1**, **4**) and separated ions (**2**, **3** and **5**) are observed. The formation of contact molecules or separated ions is mainly driven by the "fit" between the alkali metal radius and the diameter of the crown cavity. With [18]crown-6 as a well-known match for potassium and subsequent formation of a contact molecules, the combination of rubidium and [18]crown-6 has been known to afford both contact molecules and separated ions, as demonstrated with a rubidium silanide, for which two separated ions [Rb([18]crown-6)$_2$][Si-

$(SiMe_3)_3$] and one contact molecule [Rb([18]crown-6)Si-$(SiMe_3)_3$] have been identified in the asymmetric unit.[30] In accordance with this result, 1.5 equivalents of [18]crown-6 were utilized in the reaction mixture, but only the contact molecule **4** and uncoordinated crown were isolated. The formation of the separated ions **2**, **3**, and **5** is the result of the small diameter of the crown cavity relative to the alkali metal diameter, as demonstrated with the combination of either [12]crown-4 or [15]crown-5 and potassium, or [18]crown-6 and cesium. With the large alkali metals located above the cavity of the crown, the small GeH_3^- ligand is unable to provide the necessary coordinative saturation. Instead, a second crown ether binds to the metal center, independent of reagent stoichiometry. These observations agree with ion-association trends in crown ether containing silanides and germanides.[21,30] In accordance with the small size of the GeH_3^- ion relative to $Ge(SiMe_3)_3^-$, steric repulsion between the ligand and the macrocycle is much reduced, leaving room for the coordination of a THF donor in **1** and **4**.

Surprisingly, metal–germanium distances in [K([18]crown-6)Ge$(SiMe_3)_3$] (3.400(7) Å) and [Rb([18]crown-6)Ge-$(SiMe_3)_3$] (3.480(1), 3.540(2) Å)[21] are significantly shorter than in **1** (3.671(1) and 3.630(10) Å) and **4** (3.731(1) Å). This initially puzzling result, considering the small size of GeH_3^-, is explained by the unexpected GeH_3^- orientation. In fact, two out of three hydrogen atoms approach each of the metals centers with M–H distances of 3.3 Å (av) for **1** and 3.4 Å (av) for **4**. While weak, the rotation of the germyl lone pair away from the metal center enables electrostatic interactions between the negatively polarized hydrides and the alkali metal centers. Similar observations were made in a sodium alcoholate containing silyl ions.[31] In this compound, the silyl units were completely inverted, with three hydrides approaching the metal center. Theoretical studies on $LiSiH_3$ suggested that the inverted C_{3v} structure is favored by 10 kJ mol^{-1} over the conventional van't Hoff arrangement.[32] In contrast, the van't Hoff isomer of monomeric gaseous $NaSiH_3$ was calculated to be more stable than the inverted one, a result contradicted by the crystal structure of the sodium alcoholate complex mentioned above.[31] To this effect, we conducted theoretical studies to assess the relative energies of the different GeH_3^- orientations as a function of alkali metal (see below).

The geometry of the GeH_3 moiety is pyramidal, with H-Ge-H angles between 99.0° and 104.5° for **1**, 99.8° and 101.3° for **2**, 98.8 and 103.7° for **3**, and 99.4 and 102.0° for **4**. No hydrogen positions could be located for compound **5**. These values are in agreement with NMR studies on GeH_3^-;[3] the distinct pyramidal geometry is also in agreement with the above-mentioned sodium silanide moiety in which H-Si-H angles between 91 and 97° were observed. Pyramidal geometry was also observed in alkali metal trimethylsilyl, -silanides, and -germanides, with angles in the range of 100°.[21,30] While we recognize the significant uncertainty in locating hydrogen positions by using X-ray diffraction methods, a fact also supported by the large range of Ge–H distances in **1**–**4**, as well as the significant underestimation of Ge–H distances in **2** and **3**, we are confident about the assignment of pyramidal geometry. The pyramidal geometry is also in agreement with Bent's rules, indicating that the coordination of an electropositive metal increases the p character in the metal–ligand bonds, an assumption further supported by the tetrahedral geometry in germyl derivatives exhibiting an exclusively organic environment.[33–37]

As mentioned above, the detection of hydrogen positions on Ge is challenging, leading to a significant range of Ge–H distances. However, values found in **1**–**4** are rather short, likely the consequence of the limitation of conventional crystallographic analysis for locating the positions of hydrogen atoms, especially in proximity to heavier atoms, often leading into too short values. More realistic Ge–H distances (1.58 and 1.52 Å for terminal Ge-H), and 1.61 Å for Ge-H-Ge) are observed in a family of terphenyl-substituted alkali metal digermenes $[M_2\{Ge(H)Ar'\}_2]$ (M = Li, Na, K).[20] In these compounds, the reduced amount of hydrogen affords a more defined environment with hydrogen atoms that are easier to locate. The same is observed in a dimeric hydrido-(trialkylsilyl) germyllithium, in which Ge–H distances of 1.57 Å are observed.[19]

Theoretical studies

Quantum chemical calculations were employed to study the unexpected GeH_3^- binding orientations in contact structures **1** and **4**. In the absence of crystal interactions, a cation–GeH_3^- structure would be expected to conform to either that of the van't Hoff arrangement, with the anionic Ge lone pair in direct contact with the metal cation, or the GeH_3^--inverted variant, in which the three H atoms of the anion bind symmetrically to the cation. The inverted geometry was first explored by computational methods for $NaSiH_3$.[31] While the bare Na^+ and SiH_3^- were predicted to bind in the usual van't Hoff arrangement with an energy 6.5 kJ mol^{-1} lower than the inverted form at an MP4sdq/6–31G*//MP2/6–31G* level of theory, a Na^+ coordination complex (with the Na^+ at the center of a $(NaOH)_3$ six-membered ring) was found to bind SiH_3^- in an inverted C_{3v} arrangement with a 6 kJ mol^{-1} preference.[31]

In a crystal, in which numerous electrostatic interactions between complex and neighboring molecules can induce stabilization in higher energy conformations or molecular arrangements, a binding energy difference of 6 kJ mol^{-1} is almost negligible. While methods exist for the calculation of molecular crystals to accurately include all packing interactions, the unit cells of complexes **1** and **4** are prohibitively large to be studied by such means. The calculation of orientation and binding energy differences are considered only for the contact structures **1** and **4**, for which both the geometries and relative binding energies of the cation–anion complexes and the solvated cation variants can be performed at levels of theory adequate enough to generate reasonable models of the contact structure interactions. The predicted

binding orientations and relative energies are then compared with the observed orientation with specific consideration of the calculated energies as a function of both anion geometry and cation solvation.

Computational methods: Density functional theory (DFT) calculations were performed with the PC-GAMESS version[38] of the GAMESS-US quantum chemistry package[39] utilizing the B3LYP density functional,[40] 6–311G(d,p) Gaussian-type basis sets for H, C, N, and O, and Ge,[41] and the LANL2DZ effective core potentials (ECPs) for K and Rb for all structures.[42,43] Optimizations of the K–GeH_3 and (H_3N)K–GeH_3 structures were also performed by using second-order Møller–Plesset perturbation theory (MP2) with the same basis set and ECP combinations described above. As the basis for the relative energy calculations, normal mode analyses were performed on the van't Hoff and inverted C_{3v}-symmetry structures to characterize their positions on their respective potential-energy surfaces. The optimization of selected complexes and the application of symmetry restrictions to obtain various GeH_3^- conformations in the larger [18]crown-6 complexes are discussed below.

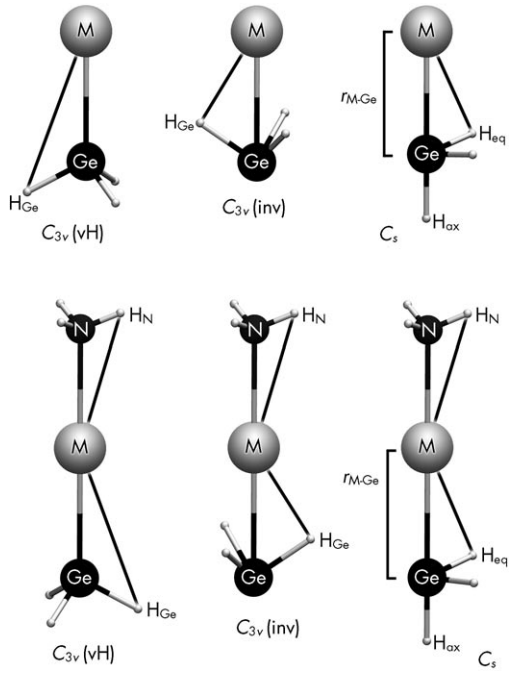

Figure 3. Geometries and atom labels for the M–GeH_3 (top) and (H_3N)M–GeH_3 (bottom) contact structures. The C_s(inv) and C_s(vH) structures are obtained by fixing the M–Ge distance (r_{M-Ge}) at the values for the C_{3v}(inv) and C_{3v}(vH) structures, respectively, and optimizing the constrained anion under C_s symmetry restrictions (see text). Graphics were generated with VMD.[44]

Computational results

$M–GeH_3$ complexes: The relative and absolute binding energies of the M–GeH_3 structures are provided in Table 3. The van't Hoff (C_{3v}(vH)), inverted (C_{3v}(inv)), and C_s symmetry forms are shown in Figure 3. The C_s structure forms the basis for two types of calculated binding interactions. The C_s structure in the M–GeH_3 and the (H_3N)M–GeH_3 structures (see next section) were geometry optimized by fixing M, Ge, and one H atom along an axis, leading to a final GeH_3^- orientation similar to the observed anion orientations in complexes **1** and **4**. Geometry optimizations of the K/Rb C_s complexes with M–Ge bond lengths fixed at the optimized van't Hoff (C_s(vH)) and inverted (C_s(inv)) C_{3v} distances were also performed. These same fixed-distance energy calculations were used in the crown ether and crown ether/NH_3 complexes (see below) for determining preferred bond lengths and relative energies.

Geometry optimizations of the M–GeH_3 complexes by both DFT and MP2 methods predict that the inverted C_{3v} structures are favored over the van't Hoff structures (Table 3). The energy differences show a two- to three-fold increase over the results for the Na–SiH_3 structure and reveal that the inverted form is favored in the absence of any additional donors. While a range of binding energies does exist for these structures, the relative changes and order of the various structures based on energy are the same, implying that the reported energy differences are important as they pertain to the accuracy of the methods to reproduce the energies. Importantly, both theoretical approaches agree on the direction of the energy changes. A few trends are worth noting in the C_{3v}(inv) and C_{3v}(vH) structures. First, all energy differences are smaller for the

Table 3. Relative orientation energies (ΔE_{Rel}) and absolute binding energies ($(H_3N)M$ or $M^+ + GeH_3^- \rightarrow (H_3N)M–GeH_3$ or $M–GeH_3 + \Delta E_{Bind}$) of the M–$GeH_3$ and (H_3N)M–GeH_3 contact structures for the five considered orientations. All energies are in kJ mol^{-1}. Structure identifiers are provided in Figure 3 and theory text.

	M–GeH_3				(H_3N)M–GeH_3			
	K LANL2DZ		Rb LANL2DZ		K LANL2DZ		Rb LANL2DZ	
	ΔE_{Rel}	ΔE_{Bind}	ΔE_{Rel}	ΔE_{Bind}	ΔE_{Rel}	ΔE_{Bind}	ΔE_{Rel}	ΔE_{Bind}
B3LYP								
C_{3v}(inv)	0.00	444.98	0.00	420.51	0.00	414.96	0.00	391.82
C_{3v}(vH)	13.14	431.84	10.89	409.62	14.89	400.07	13.16	378.66
C_s	31.52	413.46	28.68	391.83	29.04	385.92	26.53	365.29
C_s(inv)	34.64	410.34	31.84	388.66	31.39	383.57	28.70	363.13
C_s(vH)	33.83	411.15	30.74	389.77	32.05	382.91	29.68	362.15
MP2								
C_{3v}(inv)	0.00	424.55	0.00	398.10	0.00	398.80	0.00	375.81
C_{3v}(vH)	9.45	415.09	8.10	390.00	10.93	387.88	10.55	365.26
C_s	25.45	399.10	21.53	376.57	23.42	375.38	20.36	355.45
C_s(inv)	26.66	397.88	22.70	375.40	24.35	374.45	21.21	354.60
C_s(vH)	26.17	398.38	22.04	376.06	24.80	374.01	21.88	353.93

$Rb{-}GeH_3$ structures. Second, the DFT calculations always yield higher binding energy differences than the MP2 calculations. In these small $M{-}GeH_3$ structures, the energies of the C_s structures are two to three times higher than the C_{3v}(vH) energies with respect to the C_{3v}(inv) minimum energy forms, indicating a significant relative barrier to rearrangement of the anions between their C_{3v}(vH) and C_{3v}(inv) forms along a coordinate that includes the optimized C_s form. In the geometry optimizations, it is found that the M–Ge distances are nearly identical in both the C_{3v}(inv) and C_{3v}(vH) geometries, while the M–H distances are brought within nominal hydrogen–bonding range with the 1.5 Å reduction in M–H distance from anion inversion.

The possible sensitivity of the binding orientations to M–Ge separation was considered by $M{-}GeH_3$ optimization at fixed symmetries (C_{3v} and C_s) and M–Ge distances. Representative DFT and MP2 binding potentials are shown in Figure 4. Included in this figure are the binding energy differences relative to the C_{3v}(inv) forms to indicate where

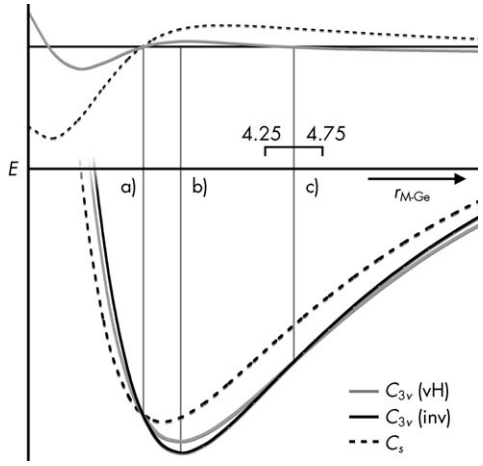

Figure 4. Representative binding potentials for the $M{-}GeH_3$ series (all contact structures follow the above trends in binding energy with M–Ge separation). a) Repulsion at reduced M–Ge distances, for which the C_s structure is the most stable form; b) global minimum energy position for the [C_{3v}(inv)] form; and c) M–Ge distance at which the C_{3v}(vH) form becomes lower in relative energy.

theory predicts that the preferred structure changes with M–Ge separation. In all cases, the van't Hoff structure becomes the more stable form at M–Ge distances in the 4.25 (K–Ge) to 4.75 Å (Rb–Ge) range. The reason for this change in preferred structure is that the anionic Ge lone pair extends further than the hydrogen atom radii, thereby only providing a preferable binding source for the metal cations when the M–H interactions have been sufficiently attenuated by increased M–Ge separation. The C_s structures are always less stable than the two C_{3v} forms, with the relative energy differences among all forms decreasing, expectedly, as each complex is separated to its dissociation limit.

$(H_3N)M{-}GeH_3$ complexes: The axial NH_3 serves as a model of cation solvation for the $M{-}GeH_3$ complexes and, in the ([18]crown-6/H_3N)$M{-}GeH_3$ complexes, they serve the role of the THF oxygen lone pair, enabling the C_{3v} symmetry optimization of these larger systems at a higher level of theory than would be practical for the asymmetric crystal THF oxygen coordination complexes **1** and **4**. The C_{3v} $(H_3N)M{-}GeH_3$ complexes were optimized with both relative orientations of the NH_3 with respect to the GeH_3^- orientation (those orientations shown in Figure 3 and the cases in which the NH_3 is rotated 180 degrees about the N-M-Ge axis). The energy differences between these two forms for each calculated structure were insignificant (less than 0.01 kJ mol^{-1} in all cases) and only the more stable orientations (as shown in Figure 3) are considered in the relative energy calculations.

The absolute and relative binding energies for the $(H_3N)M{-}GeH_3$ contact structures are provided in Table 3. The result of adding an axial NH_3 group to the $M{-}GeH_3$ complexes coincides with an increased orientation energy difference between the inverted and van't Hoff forms on the order of 2 kJ mol^{-1} over the $M{-}GeH_3$ cases. The predicted changes in M–Ge distances with NH_3 solvation are slightly larger for the B3LYP calculations (Table 4), although these MP2/B3LYP differences occur in a very small range. In comparing the absolute binding energies, the binding of the NH_3 to the cations leads to approximately 30 (B3LYP) and 25 kJ mol^{-1} (MP2) reductions in energy.

([18]crown-6)$M{-}GeH_3$ complexes: The relative binding energies for the ([18]crown-6)$M{-}GeH_3$ structures are provided in Table 4. In the C_{3v} symmetry of the van't Hoff and inverted complexes, the anion can exist in two orientations with respect to the two symmetry-unique crown ether oxygen atoms (by 60° rotation of the NH_3 about the M–Ge axis), leading to four C_{3v} forms each. The most stable forms for C_{3v}(vH) and C_{3v}(inv) are shown in Figure 5. The procedure for generating the C_s symmetry structures leads to eight unique geometries, all of which are found to occur within a 5 kJ mol^{-1} range for the K^+ complexes and 3 kJ mol^{-1} range for the Rb^+ complexes. Symmetry restrictions for the [18]crown-6/GeH_3 components led to the procedure shown in Figure 6 for the calculation of C_s symmetry minimum energy forms. The procedure is as follows.

1) The optimization of the C_{3v}(vH) form, the one for which the Ge–H distances are more similar to the C_s forms in the $M{-}GeH_3$ and $(H_3N)M{-}GeH_3$ C_s-optimized structures.
2) The crown ether is removed from this structure
3) The C_s symmetry form is optimized with M-Ge-H fixed along a single axis.
4) The crown ether is then reintroduced at its C_{3v} position relative to the metal cation
5) The anion position along the M–Ge axis is adjusted to find the lowest energy C_s symmetry form.

Structural data for the lowest energy C_{3v}(inv), van't Hoff, and C_s forms are provided in Table 4. The C_s minimum energy forms are found to lie 17 kJ mol^{-1} above the C_{3v}(inv) form for K^+ and 19 kJ mol^{-1} above the Rb^+ C_{3v}(inv) form.

Table 4. Important contact structure bond lengths [Å] for all C_{3v}(vH), C_{3v}(inv), and optimized C_s symmetry complexes. Included with the ([18]crown-6/H_3N)M−GeH_3 distances are the experimental values for complexes **1** and **4**.

			M = K				M = Rb			
			C_{3v}(vH)	C_{3v}(inv)	C_s	Exptl	C_{3v}(vH)	C_{3v}(inv)	C_s	Exptl
M−GeH_3	DFT	M−Ge	3.2217	3.2475	3.0747		3.4113	3.4496	3.2640	
		Ge−$H_{Ge/ax}$	1.5712	1.6396	1.5624		1.5728	1.6349	1.5654	
		Ge−H_{eq}			1.6062				1.6050	
	MP2	M−Ge	3.3091	3.3030	3.1399		3.5068	3.5266	3.3389	
		Ge−$H_{Ge/ax}$	1.5666	1.6270	1.5558		1.5688	1.6247	1.5590	
		Ge−H_{eq}			1.5977				1.5980	
(H_3N)M−GeH_3	DFT	M−Ge	3.2617	3.2839	3.1076		3.4547	3.4897	3.2976	
		M−N	2.9191	2.9090	2.9000		3.1627	3.1468	3.1337	
		Ge−$H_{Ge/ax}$	1.5760	1.6401	1.5665		1.5774	1.6365	1.5693	
		Ge−H_{eq}			1.6092				1.6084	
	MP2	M−Ge	3.3411	3.3251	3.1646		3.5397	3.5362	3.3576	
		M−N	2.9440	2.9359	2.9278		3.1875	3.1773	3.1665	
		Ge−$H_{Ge/ax}$	1.5700	1.6259	1.5587		1.5720	1.6236	1.5617	
		Ge−H_{eq}			1.5989				1.5992	
([18]crown-6)M−GeH_3	DFT	M−Ge	3.3869	3.4491	3.2369		3.5608	3.6095	3.3908	
		M−O_1	2.8390	2.8512	2.8390		3.0034	2.9935	3.0034	
		M−O_2	2.9662	2.9849	2.9662		3.1021	3.1077	3.1021	
		Ge−$H_{Ge/ax}$	1.5923	1.6368	1.5641		1.5908	1.6370	1.5668	
		Ge−H_{eq}			1.6032				1.6026	
([18]crown-6/H_3N)M−GeH_3	DFT	M−Ge	3.4378	3.5086	3.3076	3.630, 3.671	3.6079	3.6508	3.4279	3.731
		M−N	2.9695	2.9497	2.9695		3.1911	3.1791	3.1911	
		M−O_1	2.7987	2.8197	2.7987	2.797	2.9404	2.9385	2.9404	2.847
		M−O_2	2.9500	2.9796	2.9500	2.913	3.0744	3.0845	3.0744	2.970
		Ge−$H_{Ge/ax}$	1.5966	1.6347	1.5645		1.5936	1.6364	1.5670	
		Ge−H_{eq}			1.6027				1.6021	

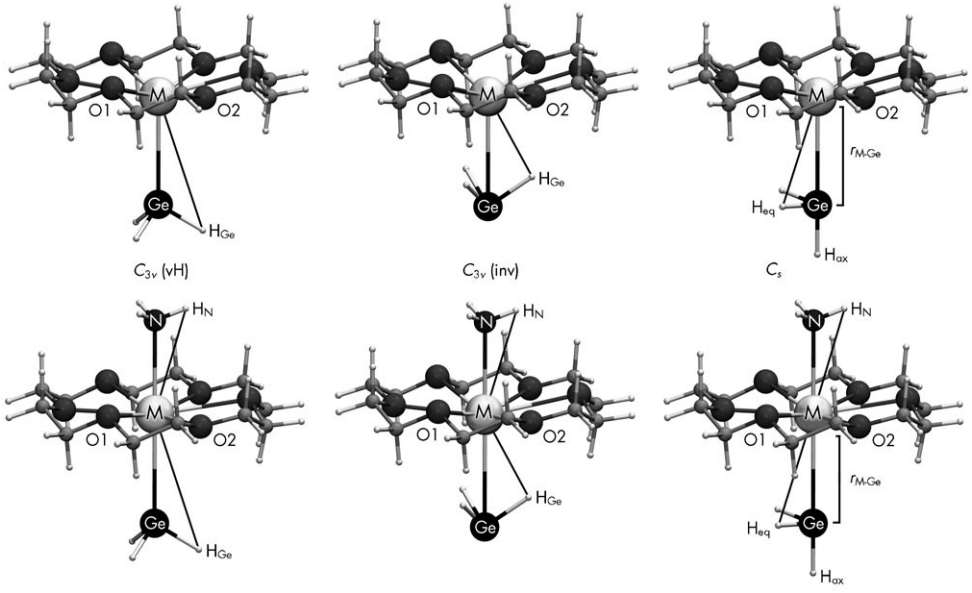

Figure 5. Geometries and atom labels for the ([18]crown-6)M−GeH_3 (top) and ([18]crown-6/H_3N)M−GeH_3 (bottom) contact structures. The C_s symmetry forms are generated according to the procedure in Figure 6 (see text). Graphics were generated with VMD.[44]

With this calculation, the energy of the C_s form for K^+ is brought within very close proximity of its highest lying C_{3v}(vH) form, while the Rb^+ remains somewhat higher than its highest energy C_{3v}(vH) form.

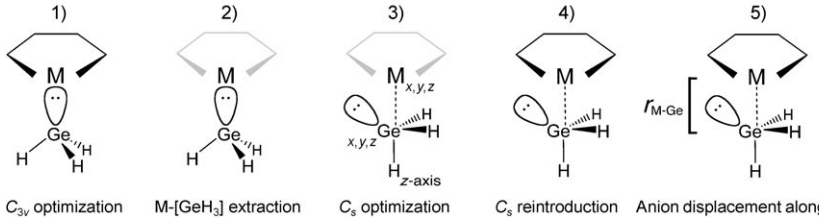

Figure 6. Procedure for generating the minimum energy C_s symmetry forms used in the relative energy calculations. See text for description of steps 1–5.

([18]crown-6/H_3N)M−GeH_3 complexes: The relative binding energies for the ([18]crown-6/H_3N)M−GeH_3 contact structures are provided in Table 5. In the C_{3v} symmetry of the

Table 5. B3LYP/6–311G(d,p)/LANL2DZ relative orientation energies (ΔE_{Rel}) of the ([18]crown-6)M−GeH_3 and ([18]crown-6/H_3N)M−GeH_3 contact structures. All energies are in kJ mol^{-1}. Structure identifiers are provided in Figure 5.

	([18]crown-6)M−GeH_3		([18]crown-6/H_3N)M−GeH_3	
	K^+ ΔE_{Rel}	Rb^+ ΔE_{Rel}	K^+ ΔE_{Rel}	Rb^+ ΔE_{Rel}
C_{3v}(inv), lowest E	0.00	0.00	0.00	0.00
C_{3v}(inv),[a] highest E	4.68	3.23	8.75	7.19
C_{3v}(vH), lowest E	14.98	16.13	13.50	16.37
C_{3v}(vH),[a] highest E	16.09	16.54	16.89	19.48
C_s(vH),[b] lowest E C_s form	18.44	20.80	13.18	18.46
C_s[c] (opt)	16.87	18.80	12.18	16.45

[a] C_{3v}(inv) and C_{3v}(vH) relative energies are reported for the highest energy forms to show the range of calculated energies for the various conformations. [b] The lowest-lying C_s symmetry form corresponding to procedure step "4" in Figure 6. [c] The lowest-lying C_s symmetry form corresponding to the displacement procedure step "5" in Figure 6.

van't Hoff and inverted complexes, eight arrangements of GeH_3^-, NH_3, and [18]crown-6 are possible (by 60° rotation of the NH_3 and/or crown ether group about the M−Ge axis) for the K^+ and Rb^+ structures. The various conformations in the C_{3v}(inv) structures occur over an 8.8 (K^+) and 7.2 kJ mol^{-1} (Rb^+) range, while the C_{3v}(vH) conformations occur over a 3.4 (K^+) and 3.1 kJ mol^{-1} (Rb^+) range. The addition of NH_3 to the K^+/Rb^+ ([18]crown-6)M−GeH_3 complexes leads to a doubling of the energy ranges for the C_{3v}-(inv) forms. The energy ranges of the C_{3v}(vH) structures are not significantly affected by the presence of the NH_3 group when the [18]crown-6/NH_3 and crown ether structures are considered together.

The C_s minimum energy forms are found to lie 12 kJ mol^{-1} above the C_{3v}(inv) form for K^+ and 16.5 kJ mol^{-1} above the Rb^+ C_{3v}(inv) form. In the case of the K^+ complex, the optimized C_s symmetry form is found to lie lower in energy than the lowest energy C_{3v}(vH) modification, while the optimized Rb^+ C_s form lies within the narrow range of its C_{3v}(vH) complexes. The prediction that the C_s form becomes this stable relative to higher symmetry forms in the most solvated K^+/Rb^+ complexes is significant as it relates to the shape of the binding potential for these isolated structures.

Even in the absence of corrections to the crown and [18]crown-6/NH_3 complexes in the optimized C_s forms (to correct for deformation of the C_{3v} crown ether to reflect [18]crown-6−GeH_3 interactions, changes in M−N NH_3 distance as the result of anion binding, etc.), the familiar C_{3v}(vH) geometry is less stable than other anion arrangements. A more complete C_s optimization (through the restriction of other atomic motions to enable the isolation of the C_s form over the predicted C_{3v}(inv) forms) would not change this outcome, and only reduce the C_{3v}(inv)→C_s energy differences beyond the significant changes found for these two complexes.

Theory discussion: The main feature of the computational studies is the significant underestimation of M–Ge distances compared to the diffraction data. Given the predicted trends in binding and orientation in the theoretical work, a 0.4 Å elongation of the M−Ge bonds in the crystal would argue for the potential energy surface corresponding to GeH_3^- orientational preferences in the crystals to be more shallow. This, coupled with the crystal environment and the packing interactions that bring other molecular fragments within vicinity of the GeH_3^- ion, would further reduce the binding energy difference between the C_{3v}(inv) and C_s forms to the point that the C_s form might, under the crystal conditions in complexes **1** and **4**, lead to a stable C_s arrangement. Accordingly, the observed GeH_3^- orientations in the crystal are excellent examples for theoretical studies directed at demonstrating the importance of crystal interactions in determining molecule geometry and conformation. The further consideration of these structures and their interactions await computational resources capable of accommodating these demanding unit cells.

Conclusion

In summary, a series of novel heavy alkali metal molecular germyl derivatives have been synthesized and structurally characterized. By adding differently sized crown ethers to the corresponding metals, contact and separated ions were obtained in the solid state. Interestingly, the contact molecules display partially inverted structures with two out of three hydrogen atoms bound to the metal center. DFT and MP2 calculations for the contact molecules reveal that solvation of the cations by the crown ether and an additional axial donor (by using NH_3 as a replacement for the crystal THF molecules) significantly affects the binding energies

and preferred binding orientations for the anion to the point at which crystal interactions could be responsible for stabilizing the nontraditional anion orientation.

Experimental Section

General considerations: All reactions were performed according standard procedures with a purified nitrogen atmosphere by utilizing either modified Schlenk techniques and/or a Braun Labmaster drybox. THF, *n*-hexane, and pentane were distilled prior to use from CaH_2 or a Na/K alloy, followed by two freeze-pump-thaw cycles. Commercially available KO*t*Bu was carefully chosen with >99% purity. $Ge(SiMe_3)_4$,[27,45] RbO*t*Bu,[46] and CsO*t*Bu[46] were prepared according to literature procedures. [18]Crown-6, [15]crown-5, [12]crown-4, and D_2O were obtained commercially. [18]Crown-6 was purified by solvation in freshly distilled diethyl ether and stirred with finely cut sodium metal for one day. After filtration from excess metal, the crown was recrystallized from hexanes. [15]crown-5 and [12]crown-4 were stored over molecular sieves (4 Å) in the dry-box. H_2O/D_2O was degassed by passing argon gas through the solution for 12 h. THF/D_2O and THF/H_2O stock solutions of known concentration were prepared shortly before use. The high reactivity of the complexes did not allow for shipping to an external laboratory for elemental analysis, even when glovebox handling was attempted. This is a well-known problem in alkali metal chemistry.[47] All ^{1}H NMR and ^{13}C NMR were recorded at room temperature on a Bruker DPX-300 spectrometer. All NMR spectra were recorded in C_6D_6 and referenced to residual solvent peaks. IR spectra were recorded as Nujol mulls using NaCl plates on a Perkin Elmer Paragon FT-IR instrument.

General procedure for the synthesis of 1–5: In a typical experiment $Ge(SiMe_3)_4$ was dissolved in THF (35 mL). This solution was then transferred into Schlenk tube containing alkali metal *tert*-butoxide dissolved in THF (35 mL). The mixture was stirred for an hour, followed by the addition of solutions of crown ether ([18]crown-6, [15]crown-5 or [12]crown-4) dissolved in THF (10 mL). To this, water (0.5 equiv; 0.009 g of water in a THF stock solution) were added very slowly through a syringe. The resulting solution was stirred for 24 h, upon which a small amount of a black precipitate was observed. The precipitate was removed by filtration, the volume of the resulting solution was reduced, and the solution layered with a small amount of pentane. Colorless crystals suitable for single-crystal analysis were obtained at −20 °C within a few days.

[K([18]crown-6)(thf)GeH_3] (1): KO*t*Bu (0.12 g, 1.1 mmol), $Ge(SiMe_3)_4$ (0.36 g, 1 mmol), and [18]crown-6 (0.26 g, 1 mmol); yield: 0.28 g, 0.63 mmol, 62.5%; m.p. 188–192 °C; ^{1}H NMR (300 MHz, C_6D_6, 25 °C, TMS): $\delta = 2.30$ (s, 3H; GeH_3), 3.23 ppm (s, 24H; CH_2, crown ether); ^{13}C NMR (75 MHz, C_6D_6, 25 °C, TMS): $\delta = 70.38$ ppm (CH_2, crown ether); IR (Nujol): $\tilde{\nu} = 2934$, 2726, 1701 (broad), 1461, 1377, 1351, 1285, 1250, 1105, 962, 888, 835, 722 cm^{-1}.

[K([15]crown-5)$_2$][GeH_3] (2): KO*t*Bu (0.12 g, 1.1 mmol), $Ge(SiMe_3)_4$ (0.36 g, 1 mmol) and [15]crown-5 (0.44 g, 2 mmol); yield: 0.38 g, 0.69 mmol, 68.6%; m.p. 204 °C (decomp); ^{1}H NMR (300 MHz, C_6D_6, 25 °C, TMS): $\delta = 3.06$ (s, 3H; GeH_3), 3.52 ppm (s, 40H; CH_2); ^{13}C NMR (75 MHz, C_6D_6, 25 °C, TMS): $\delta = 70.04$ ppm (CH_2); IR (Nujol): $\tilde{\nu} = 2922$, 1719 (broad), 1461, 1377, 1354, 1304, 1248, 1118, 1089, 1040, 939, 881, 857, 816, 722 cm^{-1}.

[K([12]crown-4)$_2$][GeH_3] (3): KO*t*Bu (0.12 g, 1.1 mmol), $Ge(SiMe_3)_4$ (0.36 g, 1 mmol) and [12]crown-4 (0.35 g, 2 mmol); yield: 0.31 g, 0.67 mmol, 67.1%; m.p. 215 °C (decomp); ^{1}H NMR (300 MHz, C_6D_6, 25 °C, TMS): $\delta = 3.06$(s, 3H; GeH_3), 3.49 ppm (s, 32H; CH_2, crown ether); ^{13}C NMR (75 MHz, C_6D_6, 25 °C, TMS): $\delta = 71.06$ ppm (CH_2); IR (Nujol): $\tilde{\nu} = 2920$, 2852, 1724 (broad), 1460, 1372, 1358, 1299, 1290, 1251, 1134, 1090, 1021, 914, 841, 817, 724, 661 cm^{-1}.

[Rb([18]crown-6)(thf)GeH_3] (4): RbO*t*Bu (0.17 g, 1 mmol), $Ge(SiMe_3)_4$ (0.36 g, 1 mmol) and [18]crown-6 (0.26 g, 1 mmol), yield: 0.36 g, 0.73 mmol, 72.5%; m.p. 176 °C (decomp); ^{1}H NMR (300 MHz, C_6D_6, 25 °C, TMS): $\delta = 2.61$ (s, 3H; GeH_3), 3.26 ppm (s, 24H; CH_2, crown ether); ^{13}C NMR (75 MHz, C_6D_6, 25 °C, TMS): $\delta = 70.63$ ppm (CH_2, crown ether). IR (Nujol): $\tilde{\nu} = 2922$, 2854, 1732 (broad), 1462, 1377, 1351, 1305, 1285, 1254, 1105, 958, 879, 835, 722 cm^{-1}.

[Cs([18]crown-6)$_2$][GeH_3] (5): CsO*t*Bu (0.22 g, 1 mmol), $Ge(SiMe_3)_4$ (0.36 g, 1 mmol) and [18]crown-6 (0.53 g, 2 mmol), yield: 0.45 g, 0.61 mmol, 61.1%; m.p. 188 °C (decomp); ^{1}H NMR (300 MHz, C_6D_6, 25 °C, TMS): $\delta = 2.98$ (s, 3H; GeH_3), 3.38 ppm (s, 48H; CH_2); ^{13}C NMR (75 MHz, C_6D_6, 25 °C, TMS): $\delta = 70.98$ ppm (CH_2); IR (Nujol): $\tilde{\nu} = 2922$, 2853, 1708 (broad), 1455, 1377, 1352, 1301, 1250, 1109, 952, 862, 838, 812 cm^{-1}.

X-ray crystallographic studies: X-ray-quality crystals for all compounds were grown as described above. Crystal mounting and data collection procedures have been described previously.[21] Hydrogen atoms on germanium (with the exception of compound **5**) were added from the Fourier maps, and germanium–hydrogen distances were fixed using the restraint DFIX. Disorder in compounds **2**–**4** was handled by including split positions for the affected groups, and included the refinement of the respective occupancies. Further details about the refinements and how disorder was handled are outlined in the Supporting Information. CCDC-295502–295506 (compounds **1**–**5**) contains the supplementary crystallographic data for this paper. These data can be obtained free of charge from The Cambridge Crystallographic Data Centre via www.ccdc.cam.ac.uk/data_request/cif.

Acknowledgements

Support from the National Science Foundation (grants CHE 0108098 and CHE-0505863) is gratefully acknowledged. Purchase of the X-ray diffractometer was made possible with grants from NSF (CHE-95-27898), the W.M. Keck Foundation and Syracuse University.

[1] C. A. Kraus, E. S. Carney, *J. Am. Chem. Soc.* **1934**, *56*, 765–768.
[2] a) G. K. Teal, C. A. Kraus, *J. Am. Chem. Soc.* **1950**, *72*, 4706–4709; b) S. N. Glarum, C. A. Kraus, *J. Am. Chem. Soc.* **1950**, *72*, 5398–5401.
[3] Von G. Thirase, E. Weiss, H. J. Hennig, H. Lechert, *Z. Anorg. Allg. Chem.* **1975**, *417*, 221–228.
[4] S. Cradock, G. A. Gibbon, C. H. Van Dyke, *Inorg. Chem.* **1967**, *6*, 1751–1752.
[5] G. H. Bauer, *Statusbericht Photovoltaik BMFT* **1990**, *25*, 1–14.
[6] T. Lobreyer, H. Oberhammer, W. Sundermeyer, *Angew. Chem.* **1993**, *105*, 587–588; *Angew. Chem. Int. Ed. Engl.* **1993**, *32*, 586–587.
[7] T. Lobreyer, W. Sundermeyer, H. Oberhammer, *Chem. Ber.* **1994**, *127*, 2111–2115.
[8] T. Lobreyer, J. Oeler, W. Sundermeyer *Chem. Ber.* **1991**, *124*, 2405–2410.
[9] G. Thirase, E. Weiss, *Z. Naturforsch. B* **1974**, *29*, 800.
[10] W. Gaede, E. Weiss, *Chem. Ber.* **1981**, *114*, 2399–2404.
[11] D. Melzer, E. Weiss, *Chem. Ber.* **1984**, *117*, 2464–2468.
[12] H. Pohlmann, E. Weiss, *Chem. Ber.* **1988**, *121*, 1427–1433.
[13] L. V. Pankratov, I. V. Zhdanovich, M. N. Bochkarev, V. I. Nevodchikov, S. Ya. Khorshev, V. N. Latyaeva, A. N. Lineva, A. S. Batsanov, Yu. T. Struchkov, *Metalloorg. Khim.* **1991**, *4*, 348–351.
[14] A. C. Filippou, J. G. Winter, G. Kociok-Koehn, I. Hinz, *J. Organomet. Chem.* **1997**, *542*, 35–49.
[15] M. N. Bochkarev, I. M. Penyagina, L. N. Zakharov, Yu. F. Rad'kov, E. A. Fedorova, S. Ya. Khorshev, Yu. T. Struchkov, *J. Organomet. Chem.* **1989**, *378*, 363–373.
[16] S. Ng, S. Hu, *Wuli Huaxue Xuebao* **2000**, *16*, 879–885.
[17] Y. Kawano, K. Sugawara, H. Tobita, H. Ogino, *Chem. Lett.* **1994**, *2*, 293–296.
[18] J. L. Vincent, S. Luo, B. L. Scott, R. Butcher, C. J. Unkefer, C. J. Burns, G. J. Kubas, A. Lledos, F. Maseras, J. Tomas, *Organometallics* **2003**, *22*, 5307–5323.

[19] T. Iwamato, J. Okita, C. Kabuto, M. Kira, *J. Am. Chem. Soc.* **2002**, *124*, 11604–11605.
[20] A. F. Richards, M. Brynda, P. P. Power, *J. Am. Chem. Soc.* **2004**, *126*, 10530–10531.
[21] W. Teng, K. Ruhlandt-Senge, *Chem. Eur. J.* **2005**, *11*, 2462–2470.
[22] J. Fischer, J. Baumgartner, C. Marschner, *Organometallics* **2005**, *24*, 1263–1268.
[23] A. G. Brook, F. Abdesaken, H. Söllradl, *J. Organomet. Chem.* **1986**, *299*, 9–13.
[24] M. Nanjo, T. Oda, K. Mochida, *J. Organomet. Chem.* **2003**, *672*, 100–108.
[25] H. Gilman, C. L. Smith, *J. Organomet. Chem.* **1968**, *14*, 91–101.
[26] C. Marschner, *Eur. J. Inorg. Chem.* **1998**, 221–226.
[27] H. Bürger, U. Goetze, *Angew. Chem.* **1968**, *80*, 192–193; *Angew. Chem. Int. Ed. Engl.* **1968**, *7*, 212–213.
[28] A. G. Brook, J. J. Chrusciel, *Organometallics* **1984**, *3*, 1317–1318.
[29] G. M. Sheldrick, SHELXTL, Program package for structure solution and refinement, BrukerAXS, Madison, WI (USA), **2003**.
[30] D. M. Jenkins, W. Teng, U. Englich, D. Stone, K. Ruhlandt-Senge, *Organometallics* **2001**, *20*, 4600–4606.
[31] H. Pritzkow, T. Lobreyer, W. Sundermeyer, N. J. R. van Eikema Hommes, P. von R. Schleyer, *Angew. Chem.* **1994**, *106*, 221–223; *Angew. Chem. Int. Ed. Engl.* **1994**, *33*, 216–217.
[32] P. von R. Schleyer, T. Clark, *J. Chem. Soc. Chem. Commun.* **1986**, 1371–1373.
[33] M. J. Barrow, E. A. V. Ebsworth, M. M. Harding, D. W. H. Rankin, *J. Chem. Soc. Dalton Trans.* **1980**, 603–606.
[34] N. W. Mitzel, U. Losehand, S. L. Hinchley, D. W. H. Rankin, *Inorg. Chem.* **2001**, *40*, 661–666.
[35] M. Brynda, M. Geoffroy, G. Bernardinelli, *Chem. Commun.* **1999**, 961–962.
[36] M. Unno, Y. Kawai, H. Matsumoto, *Heteroat. Chem.* **2001**, *12*, 238–243.
[37] F. Riedmiller, G. L. Wegner, A. Jockisch, H. Schmidbaur, *Organometallics* **1999**, *18*, 4317–4324.
[38] A. A. Granovsky, http://classic.chem.msu.su/gran/gamess/index.html
[39] M. W. Schmidt, K. K. Baldridge, J. A. Boatz, S. T. Elbert, M. S. Gordon, J. H. Jensen, S. Koseki, N. Matsunaga, K. A. Nguyen, S. Su, T. L. Windus, M. Dupuis, J. A. Montgomery, *J. Comput. Chem.* **1993**, *14*, 1347–1363.
[40] The B3LYP functional is the Becke three parameter hybrid method with LYP correlation functional, A. D. Becke, *J. Chem. Phys.* **1993**, *98*, 5648–5652.
[41] For potassium: J-P. Blaudeau, M. P. McGrath, L. A. Curtiss, L. Radom, *J. Chem. Phys.* **1997**, *107*, 5016–5021; for germanium: L. A. Curtiss, M. P. McGrath, J-P. Blandeau, N. E. Davis, R. C. Binning, Jr., L. Radom, *J. Chem. Phys.* **1995**, *103*, 6104–6113; all other atoms: R. Krishnan, J. S. Binkley, R. Seeger, J. A. Pople, *J. Chem. Phys.* **1980**, *72*, 650–654.
[42] LANL2DZ. Potassium and Rubidium: P. J. Hay, W. R. Wadt, *J. Chem. Phys.* **1985**, *82*, 270–283.
[43] Basis sets were obtained from the Extensible Computational Chemistry Environment Basis Set Database, Version 02/25/04, as developed and distributed by the Molecular Science Computing Facility, Environmental and Molecular Sciences Laboratory which is part of the Pacific Northwest Laboratory, P. O. Box 999, Richland, Washington 99352, USA, and funded by the U. S. Department of Energy. The Pacific Northwest Laboratory is a multi-program laboratory operated by Battelle Memorial Institute for the U. S. Department of Energy under contract DE-AC06–76RLO 1830. Contact David Feller or Karen Schuchardt for further information.
[44] W. Humphrey, A. Dalke, K. Schulten, Graphics were generated with VMD, *J. Mol. Graphics* **1996**, *14*, 33–38.
[45] H. Gilman, C. L. Smith, *J. Organomet. Chem.* **1967**, *8*, 245–253.
[46] M. H. Chisholm, S. R. Drake, A. A. Naiini, W. E. Streib, *Polyhedron* **1991**, *10*, 337–345.
[47] A recent review article describes this method as the most widely used for the preparation of organometallic compounds of the heavier alkali metals: D. J. Smith, *Adv. Organomet. Chem.* **1999**, *43*, 267.

Received: July 24, 2006
Published online: November 29, 2006

